

Phosphonate-Functionalized Donor Polymer as an Underlying Interlayer To Improve Active Layer Morphology in Polymer Solar Cells

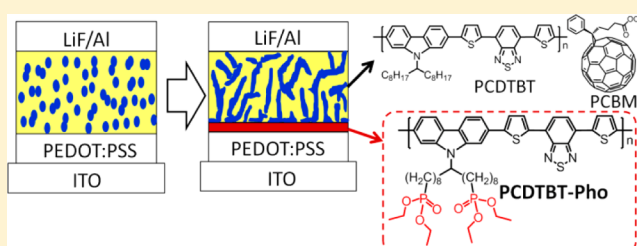
Bin Meng,^{†,‡} Yingying Fu,[†] Zhiyuan Xie,[†] Jun Liu,^{*,†} and Lixiang Wang^{*,†}

[†]State Key Laboratory of Polymer Physics and Chemistry, Changchun Institute of Applied Chemistry, Chinese Academy of Sciences, Changchun 130022, P. R. China

[‡]University of Chinese Academy of Sciences, Beijing 100039, P. R. China

S Supporting Information

ABSTRACT: A novel polymer is developed and used as underlying interlayer to improve donor polymer/acceptor material blend morphology of active layer in polymer solar cells (PSCs). The polymer poly{*N*-9-[1,17-bis-(diethylphosphonate)heptadecanyl]-2,7-carbazole-*alt*-5,5-(4,7-di-2-thienyl-2,1,3-benzothiadiazole)} (PCDTBT-Pho) is designed by attaching polar phosphonate moieties to the side chain of the donor polymer, poly[*N*-9-heptadecanyl-2,7-carbazole-*alt*-5,5-(4,7-di-2-thienyl-2,1,3-benzothiadiazole)] (PCDTBT). The pendant phosphonate moieties lead to different solubility and proper surface energy of PCDTBT-Pho. As a result, in PSC devices, the underlying PCDTBT-Pho layer facilitates the formation of bicontinuous network morphology in the active layer, makes the donor polymer enriched at the anode side, and induces the donor polymer to crystallize. These improvements contribute to improved charge separation and transport, leading to short-circuit current density enhancement by 12% and power conversion efficiency enhancement by 8% of the PSC devices. Thus, the design and application of PCDTBT-Pho indicate a novel approach to optimize active layer morphology and improve photovoltaic efficiency of PSCs.



1. INTRODUCTION

Polymer solar cells (PSCs) are receiving great attention due to their advantages of low cost, flexibility, and light weight.¹ A PSC device involves an active layer of a blend of a donor material (e.g., poly[*N*-9-heptadecanyl-2,7-carbazole-*alt*-5,5-(4,7-di-2-thienyl-2,1,3-benzothiadiazole)], PCDTBT, Scheme 1) and an acceptor material (e.g., [6,6]-phenyl-C₇₁ butyric acid methyl ester, PC₇₁BM, Scheme 1) sandwiched between an anode and a cathode. The PSC device efficiency is determined not only by the donor material and the acceptor material but also by the morphology of their blend and by the interfaces between the active layer and the electrodes.^{2,3} It has been widely accepted that the optimal morphology of the donor/acceptor blend should be a bicontinuous interpenetrating network with the phase domain size of 10–20 nm, which facilitates both exciton dissociation and charge transport.² Moreover, the optimal morphology should have the vertical ingredient distribution with the donor accumulating at the anode side and the acceptor enriched at the cathode side.² A lot of efforts have been devoted to improve morphology of donor/acceptor blend to increase PSC device efficiency. Material chemists have controlled the morphology by modifying chemical structures of donor polymers, e.g., substitution of bridge atoms in the main chain,⁴ optimization of side chains,⁵ and using specific end-capping moieties.⁶ Device physicists have developed several approaches to improve the morphology, such as thermal

annealing,⁷ solvent annealing,⁸ and using solvent additive.⁹ Good active layer morphology and high efficiency of PSCs have been achieved by modifying chemical structures and optimizing active layer processing conditions.

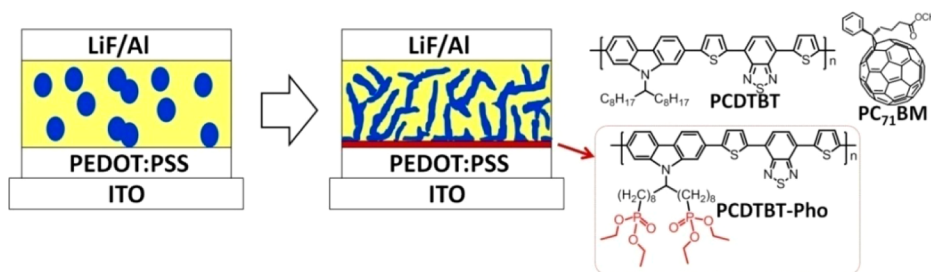
Generally, properties of the underlying layer also play an important role on the morphology of polymer blend by regulating the phase separation during the film formation.^{10,11} For PSCs, the effect of the surface energy of the underlying layer on the active layer morphology has been proved by Cho et al.¹² However, little attention has been paid to using a specific underlying layer to further improve the active layer morphology and increase the PSC device efficiency. In this article, we report the development of a morphology-inducing layer (MIL) (see Scheme 1), which is used beneath the active layer to further improve the morphology of the active layer and consequently enhance the PSC device performance.

The material in MIL is designed by introducing polar moieties to side chain of donor polymers, leading to different solubility and proper surface energy. The different solubility of the MIL material and the donor polymer enable solution processing of the active layer on top of the MIL during PSC device fabrication. Owing to the polymer backbone and the

Received: April 28, 2014

Revised: August 16, 2014

Scheme 1. Schematic of PCDTBT-Pho as MIL in PSC Devices

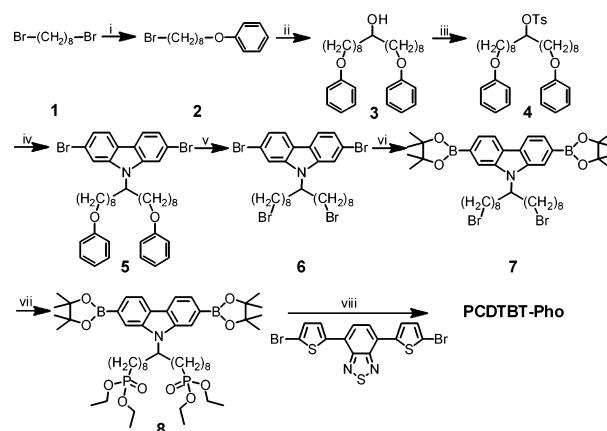


proper surface energy, the MIL can facilitate the formation of bicontinuous donor/acceptor network, make the donor polymer preferentially accumulate at the MIL surface, and induce the donor polymer to crystallize in the active layer. All these improvements in the active layer morphology are expected to increase PSC device efficiency.

PCDTBT is a typical efficient donor polymer, which can give device power conversion efficiency (PCE) of about 6%.¹³ Herein, we select PCDTBT as the donor polymer in the active layer. On the basis of our expertise on phosphonate-functionalized conjugated polymers,¹⁴ we introduce phosphonate moieties to the side chain of PCDTBT to develop the MIL material, poly{*N*-9-[1,17-bis(diethylphosphonate)heptadecanyl]-2,7-carbazole-*alt*-5,5'-(4,7-di-2-thienyl-2,1,3-benzothiadiazole)} (PCDTBT-Pho). The chemical structures of PCDTBT-Pho and PCDTBT are shown in Scheme 1. As a result, incorporation of PCDTBT-Pho as MIL in PCDTBT:PC₇₁BM device leads to much improved morphology of the active layer (see Scheme 1) and consequently short-circuit current density (J_{SC}) enhancement by 12% and PCE enhancement by 8%. We believe that the strategy of MIL can be used to further improve active layer morphology and photovoltaic performance of many high performance PSC devices.

2. RESULTS AND DISCUSSION

Scheme 2 outlines the synthetic route of PCDTBT-Pho. After 2 was synthesized by Williamson reaction of 1,8-dibromooctane and phenol, its Grignard reagent reacted with ethyl formate to afford 3. The tosylation of 3 and subsequent alkylation with 2,7-dibromocarbazole readily gave 5, which was deprotected to afford 6. The key monomer 8 was prepared by Pd-catalyzed Miyaura borylation reaction of 6 and bis(pinacolato)diboron, followed by treatment with triethyl phosphonate. Finally, the monomer 8 was copolymerized with 4,7-di(2'-bromothien-5'-yl)-2,1,3-benzothiadiazole using Suzuki polycondensation condition with Pd(PPh₃)₄ as the catalyst to afford the target polymer PCDTBT-Pho. During the polymerization, end-capping was carried out by sequential adding phenyl boric acid and bromobenzene to the reaction mixture. The polymer was purified by sequential Soxhlet extraction with acetone, toluene, and chloroform, followed by washing with hot chlorobenzene (CB). The chemical structure of PCDTBT-Pho is confirmed by ¹H NMR in deuterated *o*-dichlorobenzene (*o*-DCB) at 125 °C (Figure S3) and elemental analysis. Gel permeation chromatography (GPC) at 150 °C with 1,2,4-trichlorobenzene as the eluent indicates its number-average molecular weight (M_n) of 43 200 with polydispersity index of 3.36. According to thermogravimetric analysis (TGA), PCDTBT-Pho is stable up to 330 °C.

Scheme 2. Synthetic Route of PCDTBT-Pho^a

^aReagents and conditions: (i) phenol, K₂CO₃, acetone, reflux, 95%; (ii) Mg, THF, 50 °C, ethyl formate, 0 °C to rt, 70%; (iii) 4-toluenesulfonyl chloride, (CH₃)₃NHCl, (C₂H₅)₃N, dichloromethane, 0 °C, 100%; (iv) 2,7-dibromo-9*H*-carbazole, KOH, DMSO, 30 °C, 60%; (v) BBr₃, dichloromethane, -78 °C to rt, 61%; (vi) bis(pinacolato)diboron, Pd(dppf)Cl₂, KOAc, 1,4-dioxane, 80 °C, 85%; (vii) triethyl phosphonate, reflux, 61%; (viii) Pd(PPh₃)₄, K₂CO₃ (aq 2 M), toluene, Aliquat 336, 100 °C, 80%.

The introduction of phosphonate moieties to the side chain of PCDTBT-Pho does not obviously affect the electronic structure of the polymer backbone but greatly changes the solubility of the polymer. As shown in Figure 1a and listed in Table 1, the absorption spectra in hot *o*-DCB solution and in thin film of PCDTBT-Pho and PCDTBT are similar. The LUMO/HOMO energy levels of PCDTBT-Pho and PCDTBT (Table 1), as estimated from cyclic voltammetry (Figure 1b), are also very close. These results imply the minimal effect of the pendant phosphonate moieties on the electronic structure of the polymer backbone in PCDTBT-Pho.¹⁴ On the other hand, PCDTBT is soluble in chloroform, chlorobenzene (CB), and *o*-DCB. In contrast, PCDTBT-Pho is insoluble in chloroform and CB, and only soluble in hot *o*-DCB or hot *m*-methylphenol, indicating that the polar phosphonate moieties on the side chain change the solubility of PCDTBT-Pho. We test the solubility of PCDTBT-Pho in the solvent of CB/*o*-DCB = 1/1, which is always used in solution processing of PCDTBT:PC₇₁BM-based PSC devices. As shown in Figure 1c, the absorbance of PCDTBT-Pho thin film keeps unchanged after washing with the CB/*o*-DCB = 1/1 solvent. Therefore, the changed solubility by phosphonate moieties in PCDTBT-Pho enable us to fabricate multilayer PSC devices with PCDTBT-Pho as the underlying layer.

PSC devices were fabricated with the configuration of indium tin oxide (ITO)/poly(3,4-ethylenedioxythiophene) doped with

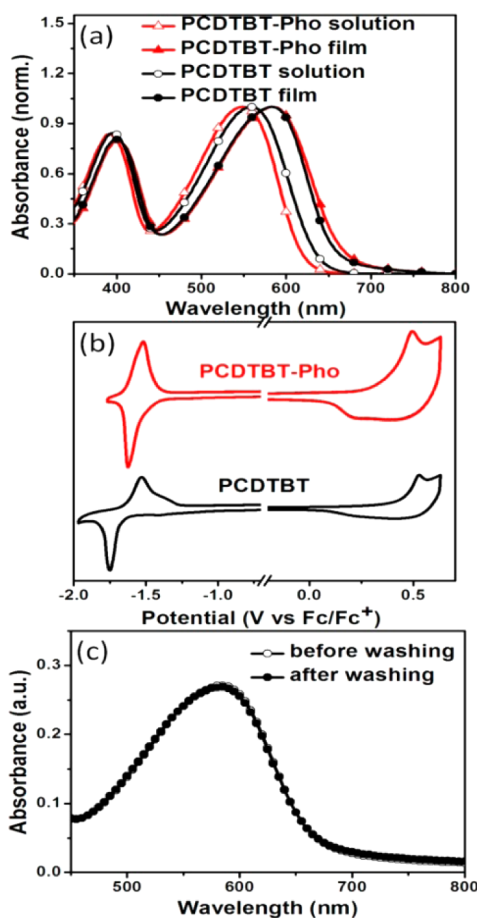


Figure 1. UV-vis absorption spectra (a) and cyclic voltammogram (b) of PCDTBT-Pho and PCDTBT. (c) Absorption spectra of a PCDTBT-Pho film without and with washing with CB/*o*-DCB = 1/1.

Table 1. Absorption Maxima, Bandgap, and LUMO/HOMO Energy Levels of PCDTBT-Pho and PCDTBT

	λ_{\max} (sol) ^a [nm]	λ_{\max} (film) [nm]	E_g^{opt} [eV]	HOMO [eV]	LUMO [eV]
PCDTBT-Pho	548	584	1.87	-5.18	-3.28
PCDTBT	559	582	1.90	-5.23	-3.19

^aDetermined in 10^{-5} M solution of *o*-DCB at 90 °C.

poly(styrenesulfonate) (PEDOT:PSS) (40 nm)/PCDTBT-Pho (1 nm)/PCDTBT:PC₇₁BM (80 nm)/LiF (1 nm)/Al (100 nm). PCDTBT-Pho was spin-coated with its solution in *o*-DCB at 120 °C, and the PCDTBT:PC₇₁BM active layer was spin-coated subsequently with the solution in CB/*o*-DCB = 1/1. A control device without the PCDTBT-Pho layer was also made for comparison. Figure 2a shows the current density–voltage (*J*–*V*) characteristics of the devices. The control device reveals the open-circuit voltage (V_{OC}) of 0.90 V, J_{SC} of 9.13 mA/cm², and fill factor (FF) of 0.68, corresponding to PCE of 5.61%. In comparison, the device with PCDTBT-Pho layer shows the V_{OC} of 0.89 V, J_{SC} of 10.18 mA/cm², FF of 0.67, and PCE of 6.03%. The two devices have virtually identical parameters, except for a 12% increase in J_{SC} for the device with PCDTBT-Pho layer. The increase in J_{SC} is confirmed by the higher external quantum efficiency (EQE) of the PCDTBT-Pho-containing device compared to the control device (Figure 2b). As shown in Table S1, the J_{SC} increase and PCE increase are

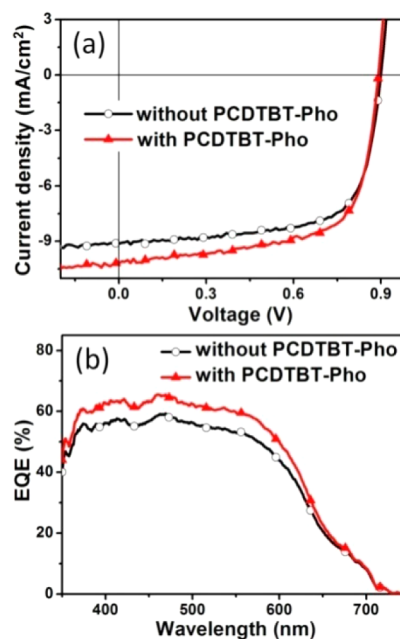


Figure 2. *J*–*V* curves (a) and EQE curves (b) of PSC devices with and without PCDTBT-Pho as MIL.

significantly out of the error of device fabrication. Indeed, other PSC devices with PCDTBT-Pho layer of different thickness also show increased J_{SC} compared to the control device (see Figure S5 and Table S1). Increase of the PCDTBT-Pho layer thickness results in decreased V_{OC} and FF, which are possibly attributed to the poor hole-transporting property of PCDTBT-Pho.

It is interesting and important to investigate the origin of the J_{SC} increase with the underlying PCDTBT-Pho layer. Considering that PCDTBT-Pho has similar LUMO/HOMO energy levels with PCDTBT and that the incorporation of thin PCDTBT-Pho layer does not increase the absorption of the active layer (see Figure S6), we pay attention to the morphology of the active layer. Transmission electron microscopy (TEM) image of the active layer in the control device (Figure 3a) reveals a rather homogeneous morphology. In contrast, the active layer in the device with the underlying PCDTBT-Pho layer (Figure 3b) shows clear fibrillar structure arising from the aggregated PCDTBT chains. The fine fibrillar structure morphology is beneficial for charge separation and charge transport in the active layer. In grazing incidence X-ray diffraction (GI-XRD) pattern of the active layer (Figure 3c), an extra peak at $2\theta = 9.5^\circ$ is observed for the active layer with underlying PCDTBT-Pho layer, implying that the PCDTBT chains are more ordered and crystalline¹⁵ possibly due to the inducing effect of the underlying PCDTBT-Pho layer. The improved crystallinity is expected to facilitate hole transport in PSCs. The inducing effect of PCDTBT-Pho is also investigated by X-ray photoelectron spectroscopy (XPS) of the bottom surface of the PCDTBT:PC₇₁BM active layer (Figure S7). The S 2p peak in XPS spectra comes from PCDTBT and can be referred as the signature of PCDTBT. The C 1s peak represents the sum of PCDTBT and PC₇₁BM. Therefore, the S 2p/C 1s peak ratio can be correlated to the content of PCDTBT in the blend.¹⁶ As listed in Table 2, the S 2p/C 1s peak ratio ($A_{\text{S } 2\text{p}}/A_{\text{C } 1\text{s}}$) is much higher for the device with PCDTBT-Pho underlying layer ($A_{\text{S } 2\text{p}}/A_{\text{C } 1\text{s}} = 0.073$) compared to the control device ($A_{\text{S } 2\text{p}}/A_{\text{C } 1\text{s}} = 0.049$), suggesting that

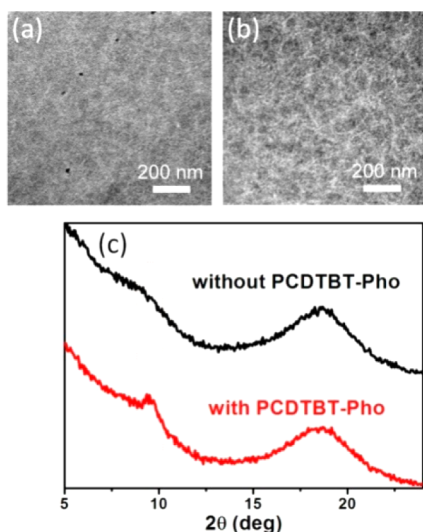


Figure 3. TEM images of the PCDTBT:PC₇₁BM active layers without (a) and with (b) PCDTBT-Pho as MIL. (c) GI-XRD patterns of the PCDTBT:PC₇₁BM active layer in the PSC devices without and with PCDTBT-Pho as MIL.

Table 2. Hole Mobility and XPS S 2p/C 1s Peak Area Ratio of the Bottom Surface of the Active Layer with and without PCDTBT-Pho Underlying Layer

	hole mobility (cm ² V ⁻¹ s ⁻¹)	S 2p/C 1s peak area ratio
with PCDTBT-Pho	2.6×10^{-5}	0.073
without PCDTBT-Pho	2.1×10^{-6}	0.049

PCDTBT is more accumulated on the PCDTBT-Pho surface than on the PEDOT:PSS surface in the control device. That means the PCDTBT-Pho underlying layer results in enrichment of the donor polymer on the anode side. This gradient distribution in the active layer (so-called vertical phase separation) is ideal for charge collection. All the TEM, XRD, and XPS results suggest improved active layer morphology with PCDTBT-Pho, which is expected to facilitate charge generation/transport. To confirm these results, we estimate the hole mobility of the PCDTBT:PC₇₁BM active layer using space charge limited current (SCLC) method according to the J - V curves of the hole-only devices (device structure: ITO/PEDOT:PSS/PCDTBT-Pho/PCDTBT:PC₇₁BM/Au). As shown in Table 2, the hole mobility with underlying PCDTBT-Pho layer ($\mu_h = 2.6 \times 10^{-5}$ cm² V⁻¹ s⁻¹) is much higher than that ($\mu_h = 2.1 \times 10^{-6}$ cm² V⁻¹ s⁻¹) of the control device without PCDTBT-Pho layer. Therefore, we believe PCDTBT-Pho is an effective MIL for PCDTBT:PC₇₁BM active layer.

We attribute the morphology regulating capability of PCDTBT-Pho to its proper surface energy and its chemical structure. It is well-known that surface energy of underlying layer can effectively alter phase separation process and consequently affect morphology.¹⁷ PCDTBT-Pho has smaller surface energy (40.5 mN m⁻¹) than that (91.6 mN m⁻¹) of PEDOT:PSS (Table S2). When PCDTBT-Pho MIL is used in PSC devices, the decreased surface energy of the underlying layer makes PCDTBT (26.8 mN m⁻¹) with smaller surface energy more favorable to accumulate on the bottom of the active layer and makes PC₇₁BM (32.8 mN m⁻¹) with higher

surface energy more favorable to enrich on the top of the active layer. Moreover, the small surface energy difference between the underlying layer and the active layer components leads to less favored dewetting process and gives rise to more pronounced phase separation. Our argument is somewhat consistent with Bulliard et al.'s report that a surface energy of about 50 mN m⁻¹ of the underlying layer gives the optimized active layer morphology and the best PSC device performance.¹² On the other hand, PCDTBT-Pho has similar polymer backbone with that of PCDTBT. When using as the underlying layer for spin-coating of the active layer, PCDTBT-Pho may induce PCDTBT to crystallize and to accumulate in the vicinity region.

3. CONCLUSIONS

In summary, we have developed a novel polymer PCDTBT-Pho with polar phosphonate moieties attached to the side chain of PCDTBT, which can be used as the underlying layer to improve the morphology of PCDTBT:PC₇₁BM active layer for better PSC device performance. Owing to its chemical structure and proper surface energy, PCDTBT-Pho facilitates the formation of biscontinuous network morphology in the active layer, makes the donor polymer enriched at the anode side, and induces the donor polymer to crystallize. These improvements contribute to improved charge separation and transport, leading to increased J_{SC} and PCE of the PSC devices. The development of MIL represents a novel strategy to further optimize active layer morphology and improve efficiency of high performance PSCs.

4. EXPERIMENTAL SECTION

Synthesis of 1-(8-Bromooctyloxy)benzene (2). In a three-necked round-bottom flask, a mixture of K₂CO₃ (311 g, 2.25 mol), phenol (53 g, 0.56 mol), 1,8-dibromooctane (460 g, 1.69 mol), and acetone (1.2 L) was heated to reflux for 15 h with vigorous stirring. After removing most of the acetone, the residual was dissolved in deionized water and dichloromethane. The organic phase was collected and washed with brine, followed by drying over anhydrous Na₂SO₄. After filtration, the solvent was removed by rotatory evaporation, and the excessive 1,8-dibromooctane was removed by distillation under reduced pressure. The residue was purified by silica gel column chromatography with petroleum ether/dichloromethane = 20/1 as eluent to afford the title compound as a white solid (151 g, 95%). ¹H NMR (300 MHz, CDCl₃), δ (ppm): 7.33–7.26 (m, 2H), 6.98–6.85 (m, 3H), 3.95 (t, $J = 6.5$ Hz, 2H), 3.41 (t, $J = 6.8$ Hz, 2H), 1.92–1.72 (m, 4H), 1.52–1.31 (m, 8H).

Synthesis of 1,17-Diphenoxyheptadecan-9-ol (3). In a three-necked round-bottom flask, a solution of 2 (76.3 g, 268 mmol) in THF (500 mL) was added dropwise to magnesium chips (6.8 g, 280 mmol), followed by stirring at 50 °C for 3 h to give the Grignard reagent. After being cooled down to room temperature, the reaction mixture was added ethyl formate (9.8 mL, 122 mmol) dropwise. The resulting reaction mixture was stirring overnight at room temperature, followed by quenching with 1 M hydrochloric acid. This mixture was extracted with diethyl ether, and the organic phase was washed with brine and dried over anhydrous Na₂SO₄. After filtration and removing the solvent under reduced pressure, the crude product was purified by silica gel column chromatography with petroleum ether/dichloromethane = 2/1 as eluent to afford the title compound as a white solid (37.2 g, 70%). ¹H NMR (300 MHz, *d*₆-DMSO), δ (ppm): 7.26 (t, $J = 7.9$ Hz, 4H), 6.92–6.88 (m, 6H), 4.22–4.00 (m, 1H), 3.93 (t, $J = 6.5$ Hz, 1H), 3.33 (br, 1H), 1.74–1.64 (m, 4H), 1.39–1.27 (m, 24H).

Synthesis of 1,17-Diphenoxyheptadecan-9-yl-4-methylbenzenesulfonate (4). To a stirred solution of 3 (36.5 g, 82.9 mmol), triethylamine (23.2 mL, 165.8 mmol), and trimethylamine hydrochloride (7.9 g, 82.9 mmol) in dichloromethane (300 mL) in an ice-

water bath, a solution of *p*-toluenesulfonyl chloride (19.8 g, 103.6 mmol) in dichloromethane (200 mL) was added dropwise. Then reaction mixture was allowed to warm to room temperature and stirred for 2 h. After work-up, the reaction mixture was washed with brine for three times, dried over anhydrous Na₂SO₄, filtered, concentrated, and dried under vacuum to afford the crude product as a yellow oil (49.3 g, 100%). The crude product was used in the next reaction without further purification.

Synthesis of *N*-9-(1,17-Diphenoxy)heptadecanyl-2,7-dibromocarbazole (5). In a three-necked round-bottom flask equipped with a pressure-equalizing dropping funnel was charged with 2,7-dibromo-9*H*-carbazole (22.5 g, 69.1 mmol), potassium hydroxide (22.8 g, 345.4 mmol), and dimethyl sulfoxide (DMSO) (100 mL). A solution of **4** (49.3 g, 82.9 mmol) in DMSO (100 mL) was added dropwise to the flask at room temperature. After being stirred for 1 day, the reaction mixture was poured into deionized water and extracted with dichloromethane for three times. The combined organic phase was washed with brine, dried over anhydrous Na₂SO₄, filtered, and concentrated. Finally, the residual was purified by silica gel column chromatography with petroleum ether/ethyl acetate = 200/1 as eluent to afford the title compound as a white solid (31.0 g, 60%). ¹H NMR (400 MHz, CDCl₃), δ (ppm): 7.92–7.86 (m, 2H), 7.69 (s, 1H), 7.53 (s, 1H), 7.36–7.29 (m, 2H), 7.27–7.24 (m, 4H), 6.92 (t, *J* = 7.3 Hz, 2H), 6.87 (d, *J* = 8.0 Hz, 4H), 4.44–4.39 (m, 1H), 3.89 (t, *J* = 6.6 Hz, 4H), 2.25–2.17 (m, 2H), 2.02–1.87 (m, 2H), 1.73–1.66 (m, 4H), 1.37–1.12 (m, 18H), 1.04–0.92 (m, 2H). ¹³C NMR (100 MHz, CDCl₃), δ (ppm): 159.07, 142.88, 139.39, 129.36, 122.32, 121.50, 121.25, 120.82, 120.40, 119.76, 119.18, 114.45, 112.12, 67.74, 56.88, 33.42, 29.17, 29.16, 29.13, 29.12, 26.62, 25.87. Anal. Calcd for C₄₁H₄₉Br₂NO₂: C, 65.87; H, 6.61; N, 1.87. Found: C, 66.13; H, 6.57; N, 1.84.

Synthesis of *N*-9-(1,17-Dibromo)heptadecanyl-2,7-dibromocarbazole (6). To a stirred solution of **5** (18.5 g, 24.7 mmol) in anhydrous dichloromethane (200 mL) at –78 °C was added dropwise a solution of boron tribromide (5.5 mL, 59.3 mmol) in dichloromethane (50 mL). After the addition, the reaction was allowed to warm to room temperature and stirred for 2 h. Then the reaction mixture was poured into deionized water and extracted with dichloromethane for three times. The combined organic phase was washed with brine, dried over anhydrous Na₂SO₄, filtered, and concentrated. The crude product was purified by silica gel column chromatography (hexane as eluent) and recrystallization in acetonitrile to afford the title compound as white crystals (10.9 g, 61%). ¹H NMR (400 MHz, CDCl₃), δ (ppm): 7.91 (m, 2H), 7.69 (s, 1H), 7.53 (s, 1H), 7.34 (t, *J* = 6.9 Hz, 2H), 4.44–4.39 (m, 1H), 3.35 (t, *J* = 6.9 Hz, 4H), 2.25–2.18 (m, 2H), 1.95–1.86 (m, 2H), 1.80–1.70 (m, 4H), 1.40–1.09 (m, 18H), 1.00–0.92 (m, 2H). ¹³C NMR (100 MHz, CDCl₃), δ (ppm): 142.91, 139.43, 122.41, 121.54, 121.30, 120.87, 119.81, 119.23, 114.50, 112.14, 56.90, 33.95, 33.44, 32.73, 29.08, 29.03, 28.48, 28.00, 26.60. MALDI-TOF (*m/z*), calcd for C₂₉H₃₉Br₄N (M⁺): 716.98. Found: 717.00. Anal. Calcd for C₂₉H₃₉Br₄N: C, 48.29; H, 5.45; N, 1.94. Found: C, 48.46; H, 5.45; N, 1.91.

Synthesis of 2,7-Bis(4,4,5,5-tetramethyl-1,3,2-dioxaborolan-2-yl)-*N*-9-(1,17-dibromo)heptadecanylcarbazole (7). A mixture of *N*-9-(1,17-dibromo)heptadecanyl-2,7-dibromocarbazole (**6**) (3.84 g, 5.32 mmol), bis(pinacolato)diboron (4.05 g, 15.96 mmol), Pd(dppf)Cl₂ (0.13 g, 0.16 mmol), KOAc (4.70 g, 47.88 mmol), and anhydrous 1,4-dioxane (50 mL) was stirred at 80 °C for 20 h under an argon atmosphere. After being cooled down, the mixture was poured into deionized water and extracted with ethyl acetate for three times. The combined organic phase was washed with brine, dried over anhydrous Na₂SO₄, and concentrated. The residual was further purified by silica gel column chromatography with petroleum ether/ethyl acetate = 50/1 as eluent to afford the title compound as a white solid (3.70 g, 85%). ¹H NMR (400 MHz, CDCl₃), δ (ppm): 8.13 (t, *J* = 9.1 Hz, 2H), 8.02 (s, 1H), 7.88 (s, 1H), 7.67 (d, *J* = 7.3 Hz, 2H), 4.72–4.67 (m, 1H), 3.33 (t, *J* = 6.9 Hz, 4H), 2.37–2.30 (m, 2H), 1.97–1.89 (m, 2H), 1.78–1.70 (m, 4H), 1.40 (s, 24H), 1.30–1.13 (m, 18H), 0.98–0.95 (m, 2H). ¹³C NMR (100 MHz, CDCl₃), δ (ppm): 141.88, 138.60, 126.00, 124.63, 120.01, 119.71, 117.98, 115.31, 83.66, 56.25, 33.89,

33.72, 32.67, 29.20, 29.00, 28.47, 27.94, 26.58, 24.91. Anal. Calcd for C₄₁H₆₃B₂Br₂NO₄: C, 60.39; H, 7.79; N, 1.72. Found: C, 60.68; H, 8.02; N, 1.74.

Synthesis of 2,7-Bis(4,4,5,5-tetramethyl-1,3,2-dioxaborolan-2-yl)-*N*-9-[1,17-bis(diethylphosphonate)heptadecanyl]carbazole (8). A mixture of **7** (3.0 g, 3.7 mmol) and triethyl phosphonate (50 mL) was refluxed with vigorous stirring for 12 h. After work-up, excessive triethyl phosphonate was removed under reduced pressure. The residual was purified by silica gel column chromatography (dichloromethane/methanol = 50/1 as eluent) to afford the title compound as a light yellow oil (2.1 g, 61%). ¹H NMR (400 MHz, CDCl₃), δ (ppm): 8.12 (t, *J* = 9.4 Hz, 2H), 8.01 (s, 1H), 7.87 (s, 1H), 7.66 (d, *J* = 5.6 Hz, 2H), 4.71–4.66 (m, 1H), 4.12–4.02 (m, 8H), 2.35–2.30 (m, 2H), 1.96–1.92 (m, 2H), 1.69–1.45 (m, 8H), 1.39 (s, 24H), 1.29 (t, *J* = 7.1 Hz, 12H), 1.26–1.10 (m, 18H), 1.00–0.94 (m, 2H). ¹³C NMR (100 MHz, CDCl₃), δ (ppm): 141.81, 138.53, 125.92, 124.55, 119.93, 119.62, 117.93, 115.27, 83.61, 61.29, 61.22, 56.22, 33.70, 30.42, 30.25, 29.26, 28.98, 28.81, 26.60, 26.15, 24.82, 22.20, 22.16, 16.36, 16.31. MALDI-TOF (*m/z*): Calcd for C₄₉H₈₃B₂NO₁₀P₂ (M⁺): 929.57. Found: 929.60. Anal. Calcd for C₄₉H₈₃B₂NO₁₀P₂: C, 63.30; H, 9.00; N, 1.51; Found: C, 62.08; H, 8.85; N, 1.44.

Synthesis of PCDTBT-Pho. In a two-necked round-bottom flask, a mixture of **8** (0.303 g, 0.326 mmol), 4,7-di(2-bromothien-5-yl)-2,1,3-benzothiadiazole (0.149 g, 0.326 mmol), Pd(PPh₃)₄ (0.005 g), Aliquat 336 (0.015 g), degassed toluene (12.0 mL), and aqueous K₂CO₃ (2.0 M, 1.0 mL) was vigorously stirred at 100 °C for 5 h under an argon atmosphere. End-capping was carried out by sequentially adding phenylboric acid (0.5 M solution in anhydrous toluene, 0.6 mL) and bromobenzene (0.4 mL) to the reaction mixture. After being cooled to room temperature, the mixture was filtered. The solid was collected, dispersed in deionized water, and ultrasonicated for 1 h. Filtration of the dispersion afford the crude product, which was further purified by Soxhlet extraction with acetone, toluene, and chloroform, followed by washing with hot chlorobenzene (CB). The dark solid was collected and dried in vacuum overnight. Yield: 0.25 g (80%). ¹H NMR (400 MHz, *d*₄-*o*-DCB, 125 °C), δ (ppm): 8.23–7.90 (br, 8H), 7.67–7.57 (br, 4H), 4.84 (br, 1H), 4.02 (br, 8H), 2.52 (br, 2H), 2.16 (br, 2H), 1.94 (br, 2H), 1.63–1.22 (m, 38H). GPC (1,2,4-trichlorobenzene, polystyrene standard, 150 °C): M_n = 43 200, PDI = 3.36. Anal. Calcd for C₅₁H₆₅N₃O₆P₂S₃: C, 62.88; H, 6.72; N, 4.31; S, 9.87. Found: C, 62.32; H, 6.63; N, 4.23; S, 9.88.

PSC Device Fabrication and Measurement. Indium tin oxide (ITO) glass substrates were cleaned by sequential ultrasonication in detergent, deionized water, acetone, and isopropyl alcohol, followed by dried at 120 °C for 30 min and treated with UV-ozone for 25 min. Then PEDOT:PSS (Baytron P Al 4083) was spin-coated on the ITO glass substrates at 5000 rpm for 40 s to give a thickness of 40 nm, followed by baking at 125 °C for 30 min. The ultrathin layer of PCDTBT-Pho was deposited on the PEDOT:PSS layer by spin-coating with its solution in *o*-DCB (0.02 or 0.05 mg/mL) at 120 °C at 2000 rpm for 40 s. Subsequently, the PCDTBT:PC₇₁BM active layer was spin-coated on the PCDTBT-Pho layer with the solution of PCDTBT (3.5 mg/mL) and PC₇₁BM (14 mg/mL) in *o*-DCB:CB = 1/1 at room temperature to give a thickness of 80 nm. Then the film was thermal annealed at 80 °C for 30 min. Finally, the device was transferred to a vacuum chamber, and LiF (1 nm)/Al (100 nm) was sequentially deposited by thermal evaporation at the pressure of about 4 × 10^{−4} Pa. The active area was 8 mm².

The *J*–*V* characteristics of PSC devices were measured using a computer-controlled Keithley 236 source meter and an oriel 150 W solar simulator with an AM 1.5G filter. The light intensity was 100 mW/cm², as determined by a calibrated silicon diode with KG-5 filter. The EQE measurement was performed under short-circuit conditions with a lock-in amplifier (SR830, Stanford Research System) at a chopping frequency of 280 Hz during illumination with a monochromatic light from a xenon lamp.

■ ASSOCIATED CONTENT

■ Supporting Information

Characterization, fabrication of hole-only devices, ^1H NMR and ^{13}C NMR spectra of the monomer **8** and PCDTBT-Pho, TGA curves, absorption of the active layer in the PSC devices, $J-V$ curves of the PSC devices with different PCDTBT-Pho layer thickness, $J-V$ curves of the hole-only devices, contact angles, and surface energies. This material is available free of charge via the Internet at <http://pubs.acs.org>.

■ AUTHOR INFORMATION

Corresponding Authors

*E-mail: liujun@ciac.ac.cn (J.L.).

*E-mail: lixiang@ciac.ac.cn (L.W.).

Notes

The authors declare no competing financial interest.

■ ACKNOWLEDGMENTS

This work was financially supported by the 973 project (No. 2014CB643504), the Nature Science Foundation of China (No. 51373165), the Strategic Priority Research Program of Chinese Academy of Sciences (No. XDB12010200), and “Thousand Talents Program” of China.

■ REFERENCES

- (1) (a) Yu, G.; Gao, J.; Hummelen, J. C.; Wudl, F.; Heeger, A. J. *Science* **1995**, *270*, 1789. (b) Thompson, B. C.; Fréchet, J. M. J. *Angew. Chem., Int. Ed.* **2008**, *47*, 58. (c) Dennler, G.; Scharber, M. C.; Brabec, C. J. *Adv. Mater.* **2009**, *21*, 1323. (d) Günes, S.; Neugebauer, H.; Sariciftci, N. S. *Chem. Rev.* **2007**, *107*, 1324. (e) Hendriks, K. H.; Heintges, G. H. L.; Gevaerts, V. S.; Wienk, M. M.; Janssen, R. A. J. *Angew. Chem., Int. Ed.* **2013**, *52*, 8341.
- (2) (a) Chen, L. M.; Hong, Z. R.; Li, G.; Yang, Y. *Adv. Mater.* **2009**, *21*, 1434. (b) Liu, F.; Gu, Y.; Jung, J. W.; Jo, W. H.; Russell, T. P. *J. Polym. Sci., Part B: Polym. Phys.* **2012**, *50*, 1018. (c) Song, H. Y.; Tong, H.; Xie, Z. Y.; Wang, L. X.; Wang, F. S. *Chin. J. Polym. Sci.* **2013**, *31*, 1117.
- (3) (a) Small, C. E.; Chen, S.; Subbiah, J.; Amb, C. M.; Tsang, S.-W.; Lai, T.-H.; Reynolds, J. R.; So, F. *Nat. Photonics* **2012**, *6*, 115. (b) He, Z. C.; Zhong, C. M.; Su, S. J.; Xu, M.; Wu, H. B.; Cao, Y. *Nat. Photonics* **2012**, *6*, 591. (c) Yip, H.-L.; Jen, A. K.-Y. *Energy Environ. Sci.* **2012**, *5*, 5994.
- (4) (a) Chen, H.-Y.; Hou, J. H.; Hayden, A. E.; Yang, H.; Houk, K. N.; Yang, Y. *Adv. Mater.* **2010**, *22*, 371. (b) Woo, C. H.; Beaujuge, P. M.; Holcombe, T. W.; Lee, O. P.; Fréchet, J. M. J. *J. Am. Chem. Soc.* **2010**, *132*, 15547. (c) Chu, T.-Y.; Lu, J.; Beaupre, S.; Zhang, Y.; Pouliot, J.-R.; Wakim, S.; Zhou, J.; Leclerc, M.; Li, Z.; Ding, J.; Tao, Y. *J. Am. Chem. Soc.* **2011**, *133*, 4250. (d) Wang, M.; Hu, X.; Liu, P.; Li, W.; Gong, X.; Huang, F.; Cao, Y. *J. Am. Chem. Soc.* **2011**, *133*, 9638. (e) Wang, E.; Wang, L.; Lan, L.; Luo, C.; Zhuang, W.; Peng, J.; Cao, Y. *Appl. Phys. Lett.* **2008**, *92*, 033307.
- (5) (a) Cabanetos, C.; Labban, A. E.; Bartelt, J. A.; Douglas, J. D.; Mateker, W. R.; Fréchet, J. M. J.; McGehee, M. D.; Beaujuge, P. M. *J. Am. Chem. Soc.* **2013**, *135*, 4656. (b) Yang, L.; Zhou, H.; You, W. *J. Phys. Chem. C* **2010**, *114*, 16793.
- (6) (a) Shim, C.; Kim, M.; Ihn, S.-G.; Choi, Y. S.; Kim, Y.; Cho, K. *Chem. Commun.* **2012**, *48*, 7206. (b) Park, J. K.; Jo, J.; Seo, J. H.; Moon, J. S.; Park, Y. D.; Lee, K.; Heeger, A. J.; Bazan, G. C. *Adv. Mater.* **2011**, *23*, 2430.
- (7) Ma, W. L.; Yang, C. Y.; Gong, X.; Lee, K. H.; Heeger, A. J. *Adv. Funct. Mater.* **2005**, *15*, 1617.
- (8) (a) Li, G.; Shrotriya, V.; Huang, J. S.; Yao, Y.; Moriarty, T.; Emery, K.; Yang, Y. *Nat. Mater.* **2005**, *4*, 864. (b) Price, S. C.; Stuart, A. C.; Yang, L.; Zhou, H.; You, W. *J. Am. Chem. Soc.* **2011**, *133*, 4625.
- (9) (a) Peet, J.; Kim, J. Y.; Coates, N. E.; Ma, W. L.; Moses, D.; Heeger, A. J.; Bazan, G. C. *Nat. Mater.* **2007**, *6*, 497. (b) Liang, Y.; Xu,

Z.; Xia, J.; Tsai, S.-T.; Wu, Y.; Li, G.; Ray, C.; Yu, L. *Adv. Mater.* **2010**, *22*, E135.

(10) (a) Heriot, S. Y.; Jones, R. A. L. *Nat. Mater.* **2005**, *4*, 782. (b) Chen, F.-C.; Lin, Y.-K.; Ko, C.-J. *Appl. Phys. Lett.* **2008**, *92*, 023307.

(11) (a) Li, C.-Y.; Wen, T.-C.; Guo, T.-F. *J. Mater. Chem.* **2008**, *18*, 4478. (b) Murray, I. P.; Lou, S. J.; Cote, L. J.; Loser, S.; Kadleck, C. J.; Xu, T.; Szarko, J. M.; Rolczynski, B. S.; Johns, J. E.; Huang, J. X.; Yu, L. P.; Chen, L. X.; Marks, T. J.; Hersam, M. C. *J. Phys. Chem. Lett.* **2011**, *2*, 3006.

(12) Bulliard, X.; Ihn, S.-G.; Yun, S.; Kim, Y.; Choi, D.; Choi, J.-Y.; Kim, M.; Sim, M.; Park, J.-H.; Choi, W.; Cho, K. *Adv. Funct. Mater.* **2010**, *20*, 4381.

(13) (a) Blouin, A.; Michaud, A.; Leclerc, M. *Adv. Mater.* **2007**, *19*, 2295. (b) Park, S. H.; Roy, A.; Beaupré, S.; Cho, S.; Coates, N.; Moon, J. S.; Moses, D.; Leclerc, M.; Lee, K.; Heeger, A. J. *Nat. Photonics* **2009**, *3*, 297.

(14) (a) Zhou, G.; Qian, G.; Ma, L.; Cheng, Y.; Xie, Z. Y.; Wang, L. X.; Jing, X. B.; Wang, F. S. *Macromolecules* **2005**, *38*, 5416. (b) Qin, C. J.; Cheng, Y.; Wang, L. X.; Jing, X. B.; Wang, F. S. *Macromolecules* **2008**, *41*, 7798. (c) Guo, X.; Qin, C. J.; Cheng, Y.; Xie, Z. Y.; Geng, Y. H.; Jing, X. B.; Wang, F. S.; Wang, L. X. *Adv. Mater.* **2009**, *21*, 3682. (d) Zhang, B. H.; Qin, C. J.; Ding, J. Q.; Chen, L.; Xie, Z. Y.; Cheng, Y. X.; Wang, L. X. *Adv. Funct. Mater.* **2010**, *20*, 2951.

(15) (a) Fang, G.; Liu, J.; Fu, Y. Y.; Meng, B.; Zhang, B. H.; Xie, Z. Y.; Wang, L. X. *Org. Electron.* **2012**, *13*, 2733. (b) Liu, J. G.; Chen, L.; Gao, B. R.; Cao, X. X.; Han, Y. C.; Xie, Z. Y.; Wang, L. X. *J. Mater. Chem. A* **2013**, *1*, 6216. (c) Jiang, G. X.; Bian, C. L.; Ding, J. Q.; Wang, L. X.; Jing, X. B.; Wang, F. S. *Chin. J. Polym. Sci.* **2013**, *31*, 787.

(16) Yao, Y.; Hou, J. H.; Xu, Z.; Li, G.; Yang, Y. *Adv. Funct. Mater.* **2008**, *18*, 1783.

(17) (a) Walheim, S.; Böltau, M.; Mlynek, J.; Krausch, G.; Steiner, U. *Macromolecules* **1997**, *30*, 4995. (b) Campoy-Quiles, M.; Ferenczi, T.; Agostinelli, T.; Etchegoin, P. G.; Kim, Y.; Anthopoulos, T. D.; Stavrinou, P. N.; Bradley, D. D. C.; Nelson, J. *Nat. Mater.* **2008**, *7*, 158.